Gridenco, Oleg ; Sebald, Kahtrin ; Tessarek, Christian ; Mehrkens, Sven ; Eickhoff, Martin ; Gutowski, Jürgen

Excitons Bound to Defect States in Two-Dimensional (2D) MoS2

Journal Article as: peer-reviewed accepted version (Postprint)

DOI of this document*(secondary publication): https://doi.org/10.26092/elib/3719

Publication date of this document: 21/02/2025

* for better findability or for reliable citation

Recommended Citation (primary publication/Version of Record) incl. DOI:

O. Gridenco, K. Sebald, C. Tessarek, S. Mehrkens, M. Eickhoff and J. Gutowski, "Excitons Bound to Defect States in Two-Dimensional (2D) MoS2," in IEEE Transactions on Nanotechnology, vol. 20, pp. 400-403, 2021, doi: 10.1109/TNANO.2021.3076574.

Excitons Bound to Defect States in Two-Dimensional (2D) MoS_2

Oleg Gridenco, Kathrin Sebald, Christian Tessarek, Sven Mehrkens, Martin Eickhoff, and Jürgen Gutowski

***Abstract*—In this work, the effect of atomic defects created by gallium ion irradiation on the optical properties of single-layer molybdenum disulfide is studied by means of micro-photoluminescence measurements. The induced defects give rise to an additional emission band located at about 170 meV below the free exciton. The micro-photoluminescence intensity of this defect-related emission band is found to be proportional to the defect density. The large spectral width suggests the presence of binding sites with different binding energies available for excitons that remain optically active up to 230 K.**

***Index Terms*—Semiconducting 2D crystals, MoS_2, exciton, micro-photoluminescence, defects.**

I. Introduction

NOWADAYS, much research is performed on atomically thin layered materials and their potential use as active material in electronic [1] and optical [2] devices as well as building blocks in functional heterostructures [3], [4]. High-quality monolayers (ML) of transition metal dichalcogenides (TMDs), with MoS_2 and WS_2 being the most prominent representatives, have been fabricated and explored, revealing strong excitonic features in the visible spectral range. The free excitons in TMD monolayers exhibit large binding energies in the order of hundreds of meV [5] due to the enhanced electron-hole interaction in 2D crystals and the reduced dielectric screening. As a result, the optical spectra are dominated by excitonic transitions even at room temperature [5], [6], in contrast to traditional three-dimensional (3D) semiconductors, in which excitonic binding energies are smaller than the thermal energy at room temperature. Besides free excitons, ML TMDs can also host localized excitons that are bound to defect states [7], [8]. Those defects are often unintentionally generated. However, point defects can be intentionally inserted by using different approaches such as ion/electron irradiation [9]–[11], plasma treatment [12], or high-temperature annealing in the presence of various gases [13], [14]. The performance of MoS_2-based devices is expected to be critically affected and altered by the structural disorder. The controlled introduction of defects gives the opportunity to create point defects. Point defects form trapping potentials in which radiative recombination of bound complexes feature good single-photon emission properties at low temperatures [15]. They emit spectrally below the free-exciton bands in TMDs.

This article reports on how focused gallium ion (Ga^+) irradiation affects the luminescence properties of thin MoS_2 layers, thus providing atomic defects with a controllable defect density. Since these materials become direct band gap semiconductors with relatively high photoluminescence (PL) intensity in the ML limit, defect effects can easily be optically monitored.

II. Methods

We have investigated ML-MoS_2 on top of SiO_2/Si substrate, see Fig. 1(a). Using micromechanical cleavage, these thin layers were exfoliated from natural bulk MoS_2 crystal using Nitto tape and transferred to a stamp. The stamp is a thin layer of commercially available viscoelastic material (Gelfilm from Gelpak) [16]. The surface of the transparent stamp was inspected under an optical microscope to select thinner flakes. This is possible due to their color contrast to the substrate under normal illumination. After a thin layer has been identified, it was possible to align it at the desired position on a Si substrate covered with 280 nm thermally grown SiO_2. The SiO_2 layer provided an efficient color contrast under white light illumination, facilitating easy identification of the thin layers. The positioning method was used to transfer the ML at desired reference points on the substrates so that afterwards, it was easier to find the ML under the electron microscope and to align it to the ion beam. Micro-photoluminescence (μ-PL) and Raman spectroscopy were used to precisely identify the monolayers. To observe μ-PL, we used a self-made confocal setup to excite MoS_2 with a 406 nm diode laser in cw mode with an excitation power of 1.9 mW. The laser spot size was $\sim$5 μm using a 50x objective with a 0.5 NA. The signal was collected using a single-grating, thermo-electrically cooled AvaSpec-ULS2048LTEC spectrometer. Low temperature (4 K) measurements were done in a liquid helium cooled cryostat. In order to introduce a controllable level of defects, the ML samples were irradiated with Ga^+ ions in a Focused Ion Beam (FIB) xT Nova Nanolab 200 System (see the sketch in Fig. 1(b)). Ion density impinging on the surface (σ) is calculated as $\sigma = It/qA$, where I is the ion current, t is exposure time, q is

Manuscript received July 31, 2020; revised March 5, 2021; accepted April 20, 2021. Date of publication April 29, 2021; date of current version May 21, 2021. This work was supported in part by the German Academic Exchange Service (DAAD), and in part by the Central Research Development Fund (CRDF) of the University of Bremen. The review of this article was arranged by the guest editors of the Special Issue for IEEE 2019 NMDC. *(Corresponding author: Oleg Gridenco.)*

Oleg Gridenco, Kathrin Sebald, Sven Mehrkens, and Jürgen Gutowski are with Semiconductor Optics Group; Institute of Solid State Physics, University of Bremen, 28359 Bremen, Germany (e-mail: gridenco@ifp.uni-bremen.de; ksebald@ifp.uni-bremen.de; mehrkens@ifp.uni-bremen.d; gutowski@ifp.uni-bremen.de).

Christian Tessarek and Martin Eickhoff are with Solid State Materials Group; Institute of Solid State Physics, University of Bremen, 28359 Bremen, Germany (e-mail: tessarek@ifp.uni-bremen.de; eickhoff@ifp.uni-bremen.de).

Digital Object Identifier 10.1109/TNANO.2021.3076574

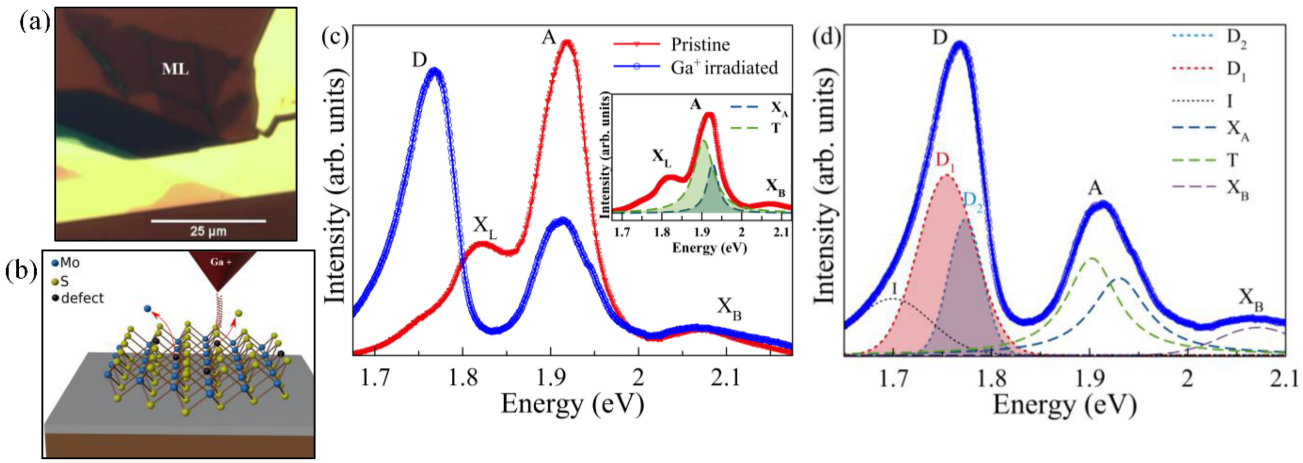

Fig. 1. (a) Optical microscope image of a MoS_2 flake, thinner part corresponds to a monolayer. (b) Schematic illustration of defects introduced by Ga^+ ions in ML-MoS_2. (c) Micro-photoluminescence spectra of the same ML-MoS_2 measured at 4 K. Pristine (red triangles) and after Ga^+ ion irradiation with a dose of 5.5 $\times$ 10^{11} ions/cm^2 (blue circled line). Dashed lines in the inset are corresponding fits for the neutral exciton (X_A) and the trion (T). (d) The same spectrum after Ga^+ ion irradiation as shown in (c) with corresponding fits (shaded areas) of D_1 (red), D_2 (light blue), and indirect band gap emission (black). Dashed lines are the corresponding fits for X_A and T, respectively.

the elementary charge, and A is the exposed area. By changing the exposure time, the ion doses can be varied between 2.5 $\times$ 10^{11} and 2.5 $\times$ 10^{13} ions/cm^2 without destroying the sample, opening the possibility to influence the number of generated defects. For higher ion doses, the μ-PL signal fell into noise level. The μ-PL spectra presented in this work were recorded on the same ML-MoS_2 flake before (pristine layer) and after Ga^+ ion irradiation and were measured under similar conditions so that a direct comparison of their optical properties is possible. For the dose-dependent measurements, several pristine monolayers were used to be irradiated with Ga^+ ion at different doses.

III. Results and Discussions

Raman measurements have been done to prove the number of layers and to confirm the presence of an ML of the investigated flake. A typical μ-PL spectrum of a pristine ML-MoS_2 as measured at 4 K is shown in Fig. 1(c) (red line). Three emission bands centered at 1.81 eV, 1.93 eV, and 2.06 eV in the μ-PL spectrum corresponding to X_L, A, and X_B are observed.

A and X_B are assigned as A-exciton and B-exciton related, respectively, where the energy separation of 130 meV is given by the spin-orbit splitting in the valence band [17]. The A excitonic band is composed of two sub-bands with energies at 1.90 eV (trion: T) and 1.93 eV (neutral exciton:X_A) [18], [19], Gaussian fits are shown as shaded areas in the inset Fig 1(c). The full width at half maximum (FWHM) yields values of 35 meV and 57 meV, respectively. Such broad linewidths are attributed to the inhomogeneous broadening due to landscape potentials (ML are not perfectly flat), imperfections, impurities, and possible excitation of more than the one-monolayer area on the flake with a relatively large laser spot in spite of using a microscope objective for laser focusing [20]. In order to suppress the inhomogeneous contribution to the excitonic linewidth, ML-TMDs were encapsulated between hexagonal boron nitride. For this case, narrow optical transition linewidths down to 2 meV at 4 K were reported [21]. The emission band X_L is generated by excitons localized to S-vacancies [22], [23], which especially applies to TMDs layers produced under ambient conditions. The energy difference between the A band and X_L band is about 110 meV, which is in good agreement with previous reports [22], [24].

Atomic defects were introduced by scanning the Ga^+ ion beam over a certain area of the MoS_2 flake (Fig. 1(b)). The defect density was changed by varying the Ga^+ ion dose from 2.5 $\times$ 10^{11} up to 2.5 $\times$ 10^{13} ions/cm^2. For higher ion doses, the μ-PL signal completely vanished. In contrast to the μ-PL spectrum measured from the pristine ML-MoS_2, after Ga^+ ion irradiation with a dose of 5.5 $\times$ 10^{11} ions/cm^2, the A band emission is suppressed, and an additional emission band D emerges at 1.76 eV in the same ML, as shown in Fig. 1(c) (blue line). This broad emission band is positioned by ΔE $\sim$ 170 meV below the neutral exciton X_A [11]. It can be fitted using three Gaussian functions (Fig. 1(c), dotted lines), suggesting that the emission is coming, first, from excitons bound two different defect types, D_1 whose emission is centered at 1.75 eV and D_2, centered at 1.77eV. This assumption can be justified since the collision between an ion and an atom can form different types of defects depending on the ion's incident angle and kinetic energy. Impurities such as topological defects, sulfur vacancies, and metallic vacancies, or a combination of those with different configurations can occur [25]. From the energy peak position, the emission band D can be assigned to atomic metal vacancies with several sulfur vacancies (V_{xMo+yS}) with different configurations, as reported in the literature [11], [26]. The linewidth of these emissions is still broad compared to the emission originating from defects introduced by He ions [11]. In contrast to that report, interactions between Ga^+ ions and the ML-MoS_2 are more destructive compared to He^+ ions since Ga^+ ions carry more charges, hence more defects can be created [27]. In addition, a large laser spot of 5 μm was used, resulting in more excited defects. Further, these defect complexes with

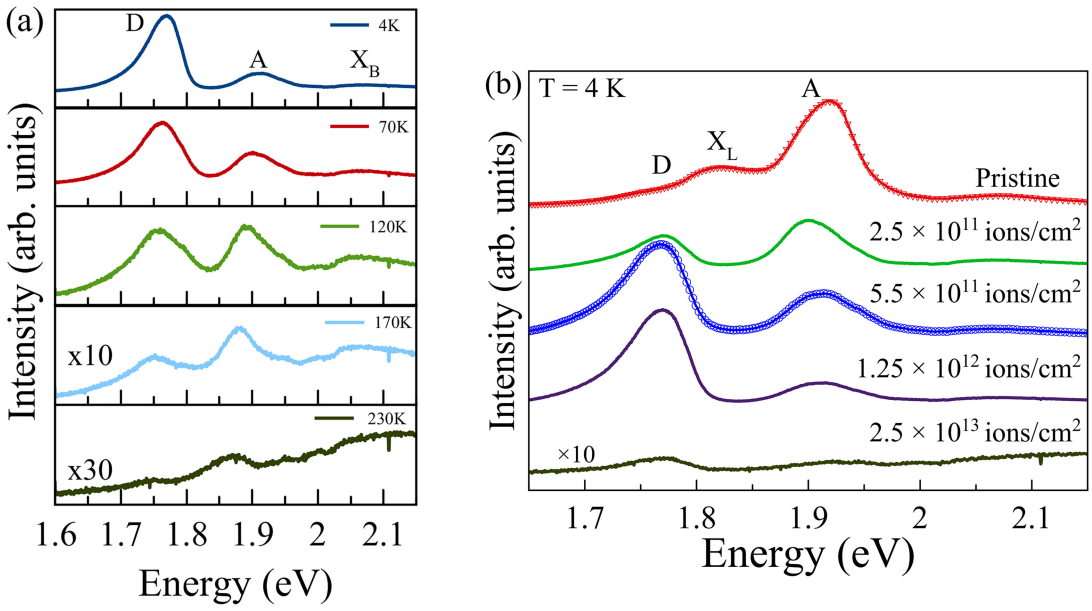

Fig. 2. (a) Temperature-dependent measurements of an ML-MoS_2 after Ga^+ ion irradiation with a dose of 5.5×10^{11} ions/cm^2. (b) Dose-dependent μ-PL measured at 4K on pristine ML-MoS_2 and Ga^+ irradiated at different ion doses from 2.5×10^{11} ions/cm^2 till 2.5×10^{13} ions/cm^2. All spectra are vertically displaced for clarity.

different configurations may possess different binding energies, thus broadening the defect-related emission band. The third Gaussian fit function (labeled I), centered at 1.69 eV, is more likely the signature of the indirect band gap as discussed in the literature [28], [29].

An important point to look at is how optically stable the localized emission remains with temperature, providing additional insights into the origin and the behavior of the defect band emissions D. Fig. 2(a) shows μ-PL spectra at temperatures between 4 K and 230 K for the sample irradiated with a dose of 5.5×10^{11} ions/cm^2. With the rising temperature, the two observed emission bands broaden and shift to lower energies. We noted that the temperature-dependent shift of defect-related emissions is very similar to the A emission band. The large spectral width of 56 meV (D_1) and 36 meV (D_2) at 4 K are an indication for inhomogeneous distribution of the exciton binding energies due to the above-mentioned potential fluctuations, and probably, to additional fluctuations of the impurity positions and neighboring. At low temperatures, the PL spectra are dominated by defect-related emissions. By increasing the temperature, the overall PL intensity decreases while the ratio between the D and A emission bands changes. For temperatures higher than 230 K, the defect-related emission band completely disappears. This quenching behavior with temperature is most likely due to activation energies that are smaller than k_BT [11] emerging due to an increase in the probability of nonradiative recombination.

The dose-dependent evolution of the emission bands is shown in Fig. 2(b). For small ion doses, the μ-PL is dominated by the A emission band. For increasing ion dose, the spectral weight ratio between the A and D emission bands changes. The emission of the bound excitons gets stronger and seems to be proportional to the defect density. However, for ion doses, $\sigma > 10^{13}$ ions/cm^2, a strong reduction of overall μ-PL intensity is observed. This might be due to the increasing destruction of the crystal lattice structure under hard ion bombardment. Another explanation discussed in the literature [30] suggests that the reduction of the μ-PL intensity can be the consequence of enhanced Auger recombination as a result of a high density of defects of the crystal and the fact that the interdefect distance approaches the size of free excitons.

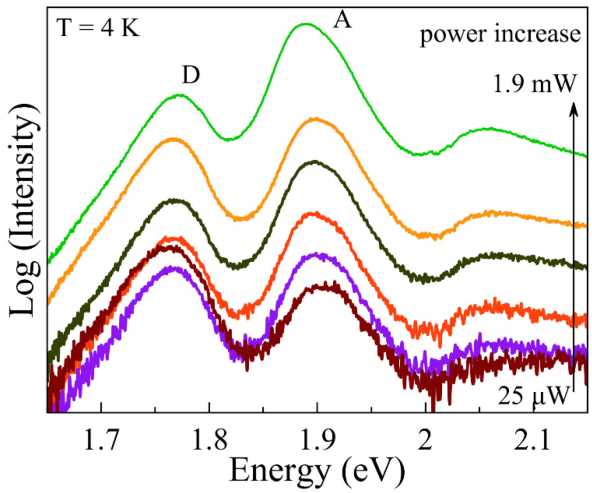

Fig. 3. Power-dependent measurements of an ML-MoS_2 after Ga^+ ion irradiation with a dose of 2.5×10^{11} ions/cm^2. The laser power incident on the sample was changed from 25 μW to 1.9 mW.

To support the assumption that the D emission band originates from excitons bound to defect states, an excitation power-dependent measurement is shown in Fig. 3 after Ga^+ ion irradiation with a dose of 2.5×10^{11} ions/cm^2. For low incident excitation power, the PL spectrum is dominated by defect-related emission. By increasing the excitation power, the intensity of the

D emission band tends to saturate, showing that the defect states become fully populated by excitons, whereas the A emission band intensity scales linearly without any sign of saturation. In comparison, for the samples irradiated with higher ion doses, the PL spectra are dominated by the defect-related emission even at high excitation power. This further supports the assumption that more defects can be created in ML-MoS_2 by increasing the ion dose.

To accurately support these interpretations, additional experiments combined with structural studies like TEM and STEM are necessary. At present, understanding and manipulation of defects on the atomic scale in TMDs remain a challenge. Further research is necessary to fully understand the dynamics of local defect formation to achieve desired localization and at controlled concentrations of defects in TMDs.

IV. Conclusion

The efficiency and ability to create optically active defects in a controllable manner induced by Ga^+ ion irradiation in MoS_2 monolayers were investigated. The defect density was controlled by changing the ion dose. Our results demonstrate that the optical properties of ML-MoS_2 can be modified after irradiation to Ga^+ ions. Additional emission bands originating from excitons bound to defect states that emit spectrally below the free-exciton line are introduced, which can be identified in the spectrum up to 230 K. We have proved that using this method, active defects can be created at a defined position in the samples.

Acknowledgment

O. G. thanks J. Dühn for help on building the μ-PL setup and S. Figge for fruitful discussion and help to operate the FIB machine.

References

[1] W. Zhu, T. Low, H. Wang, P. Ye, and X. Duan, "Nanoscale electronic devices based on transition metal dichalcogenides," *2D Mater.,* vol. 6, no. 3, Jun. 2019, Art. no. 032004.

[2] A. Pospischil and T. Mueller, "Optoelectronic devices based on atomically thin transition metal dichalcogenides," *Appl. Sci.,* vol. 6, no. 3, Mar. 2016, Art. no. 78.

[3] U. Wurstbauer, B. Miller, E. Parzinger, and A. W. Holleitner, "Light-matter interaction in transition metal dichalcogenides and their heterostructures," *J. Phys. D: Appl. Phys.,* vol. 50, no. 17, Mar. 2017, Art. no. 173001.

[4] Y. Shimazaki, I. Schwartz, K. Watanabe, T. Taniguchi, M. Kroner, and A. Imamoglu, "Strongly correlated electrons and hybrid excitons in a moiré heterostructure," *Nature,* vol. 580, no. 7804, pp. 472–477, Apr. 2020.

[5] G. Wang *et al.*, "Colloquium: Excitons in atomically thin transition metal dichalcogenides," *Rev. Modern Phys.,* vol. 90, no. 2, Apr. 2018, Art. no. 021001.

[6] K. F. Mak, K. He, C. Lee, G. H. Lee, J. Hone, and T. F. Heinz, "Tightly bound trions in monolayer MoS_2," *Nature Mater.*, vol. 12, no. 3, pp. 207–211, Mar. 2013.

[7] P. Shen *et al.*, "Pressure-dependent strong photoluminescence of excitons bound to defects in WS_2 quantum dots," *Adv. Mater. Interfaces,* vol. 5, Jun. 2018, Art. no. 1800305.

[8] V. Carozo *et al.*, "Optical identification of sulfur vacancies: Bound excitons at the edges of monolayer tungsten disulfide," *Sci. Adv.,* vol. 3, no. 4, Apr. 2017, Art. no. e1602813.

[9] T. Xu, Y. Shen, K. Yin, and L. Sun, "Precisely monitoring and tailoring 2D nanostructures at the atomic scale," *APL Mater.,* vol. 7, no. 5, Apr. 2019, Art. no. 050901.

[10] M. Schleberger and J. Kotakoski, "2D material science: Defect engineering by particle irradiation," *Materials,* vol. 11, no. 10, Aug. 2018, Art. no. 1885.

[11] J. Klein *et al.*, "Site-selectively generated photon emitters in monolayer MOS_2 via local helium ion irradiation," *Nat. Commun.,* vol. 10, Jun. 2019, Art. no. 2755.

[12] H. Nan *et al.*, "Strong photoluminescence enhancement of MOS_2 through defect engineering and oxygen bonding," *ACS Nano,* vol. 8, no. 6, pp. 5738–5745, May 2014.

[13] L. Su, Y. Yu, L. Cao, and Y. Zhang, "In situ monitoring of the thermal-annealing effect in a monolayer of MOS_2," *Phys. Rev. Appl.,* vol. 7, Oct. 2016, Art. no. 034009.

[14] M. Precner *et al.*, "Evolution of metastable defects and its effect on the electronic properties of MOS_2 films," *Sci. Rep.,* vol. 8, Apr. 2018, Art. no. 6724.

[15] P. Tonndorf *et al.*, "Single-photon emission from localized excitons in an atomically thin semiconductor," *Optica,* vol. 2, no. 4, pp. 347–352, Apr. 2015.

[16] A. Castellanos-Gomez *et al.*, "Deterministic transfer of two-dimensional materials by all-dry viscoelastic stamping," *2D Mater.,* vol. 1, no. 1, Apr. 2014, Art. no. 011002.

[17] A. Kormanyos *et al.*, "k·p theory for two-dimensional transition metal dichalcogenide semiconductors," *2D Mater.*, vol. 2, Apr. 2015, Art. no. 022001.

[18] J. Wierzbowski *et al.*, "Direct exciton emission from atomically thin transition metal dichalcogenide heterostructures near the lifetime limit," *Sci. Rep.,* vol. 7, Sep. 2017, Art. no. 12383.

[19] F. Cadiz *et al.*, "Well separated trion and neutral excitons on superacid treated MOS_2 monolayers," *Appl. Phys. Lett.,* vol. 108, no. 25, Jun. 2017, Art. no. 251106.

[20] G. Moody *et al.*, "Intrinsic homogeneous linewidth and broadening mechanisms of excitons in monolayer transition metal dichelcogenides," *Nat. Commun.,* vol. 6, Sep. 2015, Art. no. 8315.

[21] F. Cadiz *et al.*, "Excitonic linewidth approaching the homogeneous limit in MOS_2-Based van der waals heterostructures," *Phys. Rev. X,* vol. 7, no. 2, Apr. 2017, Art. no. 021026.

[22] S. Tongay *et al.*, "Defects activated photoluminescence in two-dimensional semiconductors: Interplay between bound, charged, and free excitons," *Sci. Rep.,* vol. 3, Sep. 2013, Art. no. 2657.

[23] H.-P. Komsa and A. V. Krasheninnikov, "Native defects in bulk and monolayer MOS_2 from first principles," *Phys. Rev. B,* vol. 91, Mar. 2015, Art. no. 125304.

[24] T. Korn, S. Heydrich, M. Hirmer, J. Schmutzler, and C. Schuller, "Low-temperature photocarrier dynamics in monolayer MOS_2," *Appl. Phys. Lett.,* vol. 99, no. 10, Sep. 2011, Art. no. 102109.

[25] M. Ghorbani-Asl, S. Kretschmer, D. E. Spearot, and A. V. Krasheninnikov, "Two-dimensional MOS_2 under ion irradiation: From controlled defect production to electronic structure engineering," *2D Mater.,* vol. 4, no. 2, Apr. 2018, Art. no. 025078.

[26] J. P. Thiruraman *et al.*, "Angstrom-size defect creation and ion transport through pores in single-layer MOS_2," *Nano Lett.*, vol. 18, no. 3, pp. 1651–1659, Feb. 2018.

[27] J. Buchheim, R. M. Wyss, I. Shorubalko, and H. G. Park, "Understanding the interaction between energetic ions and freestanding graphene towards practical 2D perforation," *Nanoscale,* vol. 8, no. 15, pp. 8345–8354, Mar. 2016.

[28] J. Peto *et al.*, "Moderate strain induced indirect bandgap and conduction electrons in MOS_2 single layers," *npj 2D Mater. Appl.,* vol. 3, no. 39, Oct. 2019.

[29] E. Blundo *et al.*, "Evidence of the direct-to-indirect band gap transition in strained two-dimensional WS_2, MOS_2, and WSe_2," *Phys. Rev. Res.,* vol. 2, no. 2, Jan. 2020, Art. no. 012024(R).

[30] J. Klein *et al.*, "Robust valley polarization of helium ion modified atomically thin MOS_2," *2D Mater.*, vol. 5, no. 1, Nov. 2017, Art. no. 011007.